AJNR

Visualization of Intracranial Aneurysms Treated with Woven EndoBridge Devices Using Ultrashort TE MR Imaging

Daniel Toth, Stefan Sommer, Riccardo Ludovichetti, Markus Klarhoefer, Jawid Madjidyar, Patrick Thurner, Marco Piccirelli, Miklos Krepsuka, Tim Finkenstädt, Roman Guggenberger, Sebastian Winklhofer, Zsolt Kulcsar and Tilman Schubert

Visualization of Intracranial Aneurysms Treated with Woven EndoBridge Devices Using Ultrashort TE MR Imaging

Daniel Toth, Stefan Sommer, [ID]Riccardo Ludovichetti, [ID]Markus Klarhoefer, Jawid Madjidyar, Patrick Thurner, [ID]Marco Piccirelli, Miklos Krepsuka, Tim Finkenstädt, [ID]Roman Guggenberger, [ID]Sebastian Winklhofer, [ID]Zsolt Kulcsar, and [ID]Tilman Schubert

ABSTRACT

BACKGROUND AND PURPOSE: Assessing the treatment success of intracranial aneurysms treated with Woven EndoBridge (WEB) devices using MRI is important in follow-up imaging. Depicting both the device configuration as well as reperfusion is challenging due to susceptibility artifacts. We evaluated the usefulness of the contrast-enhanced 3D ultrashort TE (UTE) sequence in this setting.

MATERIALS AND METHODS: In this prospective study, 12 patients (9 women) with 15 treated aneurysms were included. These 12 patients underwent 18 MRI examinations. Follow-up UTE-MRI controls were performed on the same 3T scanner. We compared the visualization of device configuration, artifact-related virtual stenosis of the parent vessel, and the WEB occlusion scale in 3D isotropic UTE-MRI postcontrast with standard TOF-MRA with contrast-enhancement (CE) and without IV contrast as well as DSA. Two interventional neuroradiologists rated the images separately and in consensus.

RESULTS: Visualization of the WEB device position and configuration was rated superior or highly superior using the UTE sequence in 17/18 MRIs compared with TOF-MRA. Artifact-related virtual stenosis of the parent vessel was significantly lower in UTE-MRI compared with TOF and CE-TOF. Reperfusion was visible in 8/18 controls on DSA. TOF was able to grade reperfusion correctly in 16 cases; CE-TOF, in 16 cases; and UTE, in 17 cases.

CONCLUSIONS: Contrast-enhanced UTE is a novel MRI sequence that shows benefit compared with the standard sequences in noninvasive and radiation-free follow-up imaging of intracranial aneurysms treated using the WEB device.

ABBREVIATIONS: AcomA = anterior communicating artery; BA = basilar artery; CE = contrast enhancement; CEA = contrast-enhanced angiography; PcomA = posterior communicating artery; UTE = ultrashort TE

The treatment of wide-neck aneurysms, which constitute up to 54% of intracranial aneurysms,[1,2] may be challenging due to the proximity of branching vessels.[3] Besides surgical clipping, several endovascular methods have been used, including coiling with temporary or permanent stent assistance or deployment of a flow-diverting stent. One of the more recent options is the Woven EndoBridge device (WEB; MicroVention/Terumo), an intrasaccular flow-disrupting device, which was introduced for clinical use in 2011.[4] WEB devices have been successfully used in a number of locations, including the anterior communicating artery (AcomA), the MCA, the ICA, and the basilar artery (BA).

Equivalent to other intracranial aneurysm treatment options, interval follow-up imaging for monitoring of residual filling recurrence of the aneurysm and complications such as occlusion of branching vessels is mandatory. The gained information is necessary for planning further follow-up intervals, adjusting anticoagulant medication regimens, and determining the need for re-treatment.[5,6] Due to the compact microwire braiding, which makes up the WEB device, the information gained with CT and MRI will be limited by beam-hardening and susceptibility artifacts, respectively.[7,8] Ideally, MRA would be able to show the configuration of the WEB device, which may experience infolding at the base, aneurysm recanalization along the aneurysm walls, and, rarely, dislocation. Furthermore, branch vessels at the aneurysm base may be obstructed by the WEB device if it is not properly sized. Aneurysms treated with WEB devices may show different kinds of recanalization compared with coiled aneurysms described by the WEB Occlusion Scale.[9]

Typical MRA sequences used in this setting are noncontrast TOF, contrast-enhanced angiography (CEA), and time-resolved CEA.[8,10] Some institutions also use contrast-enhanced TOF, which

SUMMARY

PREVIOUS LITERATURE: Previous studies have explored the limitations of conventional MRI sequences in visualizing intracranial aneurysms treated with endovascular devices due to susceptibility artifacts. TOF-MRI, including CE-TOF, often has artifacts that obscure critical details of the device and adjacent vessels. Studies have shown the potential of UTE-MRI to mitigate these issues, offering better visualization of metal implants used in various aneurysm treatments such as stents and coils through reduced susceptibility artifacts.

KEY FINDINGS: UTE-MRI provides superior visualization of WEB devices and adjacent vessels compared with TOF-MRA, with significantly less artifact-related virtual stenosis and accurate assessment of aneurysm occlusion.

KNOWLEDGE ADVANCEMENT: This study demonstrates that UTE-MRI enhances follow-up imaging for intracranial aneurysms treated with WEB devices, improving the ability to assess device configuration and vessel patency, potentially guiding better clinical management.

offers a higher SNR, especially in small vessels.[11] However, visualization of the device and adjacent vessels with conventional MRI is limited due to the susceptibility artifacts, especially of the proximal and distal markers. Ultrashort TE (UTE)-MRI may overcome this limitation due to the markedly reduced susceptibility to metal artifacts. Several studies have demonstrated the usefulness of a UTE sequence for follow-up of intracranial aneurysms treated with stents, coils, and flow diverters using arterial spin-labelling–based TOF with zero TE.[12-15]

In this study, we assessed the usefulness of a fast radial 3D UTE research application sequence for follow-up of intracranial aneurysms treated with a WEB device regarding visualization of the device, potential recanalization, and adjacent structures.

MATERIALS AND METHODS

This prospective pilot study was designed to evaluate the usefulness of a 3D UTE research application sequence using radial center-out sampling in patients having undergone aneurysm treatment using the WEB device. The application of this sequence for research purposes was approved by the local institutional review board (Kantonale Ethikkommission).

We prospectively included 12 consecutive patients who had undergone therapy of an intracranial aneurysm using the WEB device between November 2020 and May 2022. These patients were imaged either within 24 hours after WEB implantation or during scheduled routine clinical and MRI follow-up 12 months after WEB implantation. All patients were given an explanation of the nature of the investigation prior to the MRI, and written informed consent was obtained. All methods were applied in accordance with relevant guidelines and regulations (Declaration of Helsinki). In the study database, all personal information was deleted to protect privacy.

For these patients, we collected standard demographic data including sex and age as well as data on any intracranial procedures performed, including the date, vessel site, and device used for the WEB intervention.

Imaging

The 3D isotropic UTE sequence under investigation uses the following scan parameters: TR/TE: 4.6/0.04 ms; flip angle: 5 degrees; field of view: 230×230 mm^2; matrix: 384×384; slice thickness: 0.6 mm; acquisition time: 2 minutes 58 seconds. The images were acquired in the axial plane.

We performed our standard protocol used for routine follow-up of patients with aneurysms at our institution: 3D FLAIR, T2 TSE, DWI, TOF angiography, TOF angiography after IV administration of 7 mL of gadobutrol (Gadovist; Bayer) = contrast-enhancement (CE)-TOF, Additionally, the UTE sequence was performed after contrast administration. The scan parameters for our standard TOF sequence are the following: TR/TE: 3.43/20 ms; flip angle: 25 degrees; field of view: 210×210 mm^2; matrix, 224×320; slice thickness: 0.6 mm; and acquisition time: 5 minutes 11 seconds.

All MRI exams were performed on the same 3T Magnetom Skyra Scanner (Siemens Healthineers) in all patients using a 32-channel head coil. The MRIs were performed between November 2020 and May 2022.

Invasive Imaging. Standard biplanar DSA was performed during WEB implantation and during routine follow-up. In addition, flat panel detector CT with intra-arterial contrast administration was performed as well during WEB implantation and follow-up. DSA images were acquired within 24 hours of the MRI on one of our 2 angiography suites: Axiom Artis (Siemens Healthineers) or Azurion (Philips Healthcare).

Image Analysis. Two interventional radiologists (T.S. and D.T., with 16 and 10 years of experience, respectively, in radiology, as well as 9 and 5 years, respectively, in interventional neuroradiology) independently reviewed all imaging as an anonymized data set in the PACS. The readers used MPRs in standard axial, sagittal, and coronal as well custom planes for the MRIs and modified window widths and levels as needed on all images, including DSA. To avoid recall bias, we adhere to an interval of at least 30 days between reading the different data sets (TOF/TOF-CE, UTE. and DSA).

Artifact-Related Virtual Stenosis

Artifact-related virtual stenosis of the parent vessel was assessed by performing an automated vessel analysis along the parent vessel including the base of the aneurysm (Fig 1). The syngo.via vessel analysis tool was used (Siemens Healthineers). We extracted the minimum and maximum vessel diameter from the vessel analysis and compared it between MRI modalities.
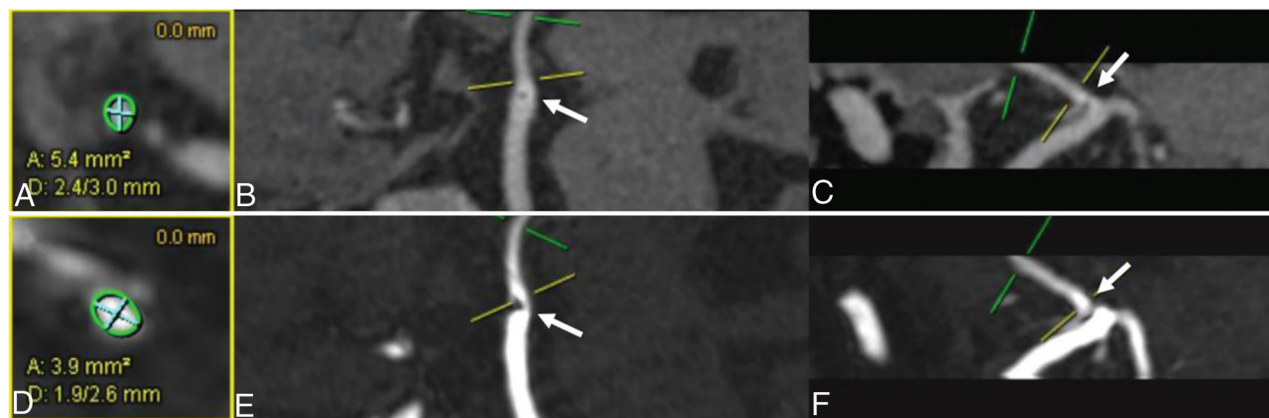
FIG 1. Representative case of the virtual stenosis analysis: The minimal diameter is calculated as the transverse vessel surface in square millimeters (*A, B, C:* UTE-MRI, *D, E, F:* TOF-MRA). Note the smaller cross-sectional surface vessel in TOF-MRA (*D–F*) caused by the numerous artifacts of the WEB-detachment zone (*arrows*) compared with UTE MRI (*A–C*).

Table 1: Summary of demographics and aneurysm location of 12 patients with 15 aneurysms

Summary	
Age (yr)	65 (8.5)
Female sex	9 (75%)
Aneurysm location	
AcomA	6
BA	6
MCA	2
PcomA	1

Virtual stenosis was calculated as follows:

$$\left(1 - \frac{Min\ VD}{Max\ VD}\right) \times 100,$$

where MinVD refers to the minimum vessel diameter and MaxVD refers to the maximum vessel diameter.

Aneurysm Occlusion

Occlusion of the treated aneurysms was evaluated according to the WEB occlusion scale (0, 0,' 1, 2, 3, 1 + 3).[16] This was assessed separately on the TOF, CE-TOF, UTE and DSA images. After individual ratings, we performed consensus reading for all cases.

Visualization of the WEB Device and Adjacent Vessels

The visibility of the WEB device configuration and the visualization of parent vessels were rated on a 3 point Likert scale of 1—3 (3: excellent, 2: good, 1: poor). The criteria were the ability to visualize the following: 1) both markers of the WEB device in order to facilitate understanding of device orientation, 2) the configuration of the WEB device in order to detect changes in configuration over time, and 3) the depiction of the borders of the WEB device towards the lumen of the adjacent vessels to detect protrusion and aneurysm recanalization. If all criteria were met, a score of 3 was applied; if 1 criterion was not satisfactorily visualized, a score of 2; and if $\geq$2 criteria were poorly or not visible, a score of 1 was given. This rating was performed on the TOF images and the UTE images separately and in consensus (Table 2). The WEB configuration, orientation, and the relationship of the device to

Table 2: WEB and parent vessel visibility was rated on a 3-point Likert scale of 3 to 1 (3: excellent, 2: good, 1: poor)

MRI Scan	WEB Visibility Rating (UTE)	WEB Visibility Rating (TOF)	Parent Vessel Visibility (UTE)	Parent Vessel Visibility (TOF)
1	3	2	2	3
2	3	2	3	2
3	3	1	2	2
4	3	1	3	2
5	3	2	3	2
6	3	1	3	3
7	3	1	3	2
8	3	1	3	2
9	3	1	3	2
10	2	2	3	2
11	3	1	3	2
12	2	1	3	3
13	3	1	2	2
14	2	1	3	0
15	2	1	3	2
16	3	2	3	3
17	3	2	2	2
18	3	1	3	1

the parent vessel were compared with the criterion standard DSA (2D and 3D DSA).

Statistical Analysis

Interreader reliability was assessed using the Cohen κ statistics (0.1–0.2: slight agreement, 0.21–0.4: fair agreement, 0.41–0.6: moderate agreement, 0.61–0.8: substantial agreement, 0.81–0.99: near-perfect agreement).

Visibility of the WEB device and adjacent vessel measurements of UTE and TOF were compared using a Wilcoxon signed-rank test.

Minimal vessel diameter results from the vessel analysis along the base of the aneurysm were assessed by 2-sided Student *t* tests.

Consensus reading results of WEB recanalization visualized in UTE, TOF, and TOF postcontrast were compared with the DSA results using a Wilcoxon signed-rank test.

Statistical significance levels were set at *P* < .1 due to the low number of patients.
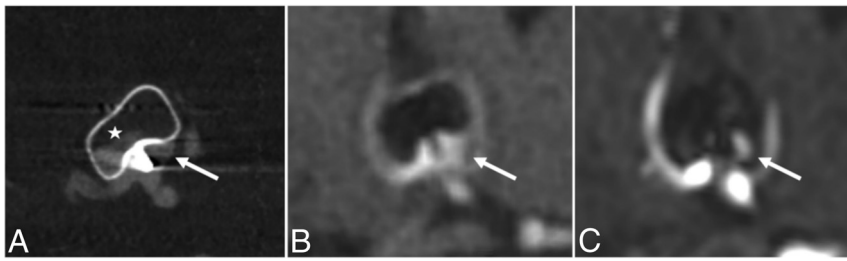
FIG 2. Follow-up of an incidental AcomA aneurysm treated with a WEB device. Note the deformation of the WEB excellently depicted in flat-panel detector CT (*A, arrow*) and UTE-MRI (*B, arrow*). The shape of the WEB cannot be clearly visualized using TOF-MRA after contrast administration (*C, arrow*). The perfusion within the WEB device, however, cannot be visualized with an MRI technique (*asterisk, A*) due to radiofrequency shielding effects.
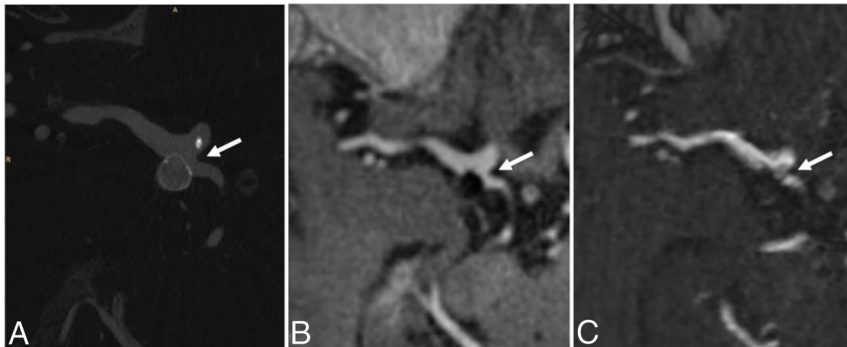

FIG 3. A PcomA aneurysm treated with the WEB. The origin of the PcomA is well-visualized in flat-panel detector CT with an intra-arterial contrast injection (*A, arrow*) and UTE-MRI (*B, arrow*). In TOF-MRA with contrast (*C*), the WEB detachment zone creates an artifact that does not allow clear visualization of the PcomA origin (*arrow*).
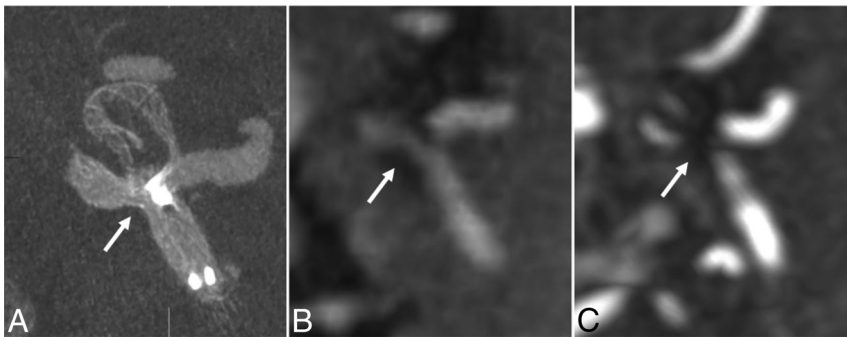

FIG 4. Example of an AcomA aneurysm treated with WEB and stent in the A1–A2 junction due to protrusion of the WEB after detachment. Note the visualization of the patent stent lumen in flat-panel detector CT with intra-arterial contrast injection (*A, arrow*) and UTE-MRI (*B, arrow*). In contrast-enhanced TOF-MRA (*C*), the in-stent lumen adjacent to the proximal marker cannot be visualized (*arrow*).

RESULTS

We included 12 consecutive patients with 15 treated aneurysms. These 12 patients underwent 18 MRI examinations. TOF-MRA was available in all MRI examination, TOF-CE was available in 17 of 18 examinations, and UTE, in all MRI examinations. DSA was available in all imaging visits.

The demographics are summarized in Table 1. The median age was 65 years (range, 53–78 years). Six aneurysms were located in the AcomA, 6 in the BA, 2 in the MCA, 1 on the

right, 1 on the left side) and 1 at the origin of the posterior communicating artery (PcomA).

The WEB devices used ranged from 4.5×3 mm to 10×5 mm with an average diameter of 7.8 mm and an average height of 4.2 mm. Coils were used in addition to the WEB device in 2 cases, and a self-expandable stent (Neuroform Atlas; Stryker Neurovascular) was used in 1 case.

Thirteen MRI examinations were performed within 24 hours after WEB implantation. Five MRI examinations were performed during follow-up. Of these, 3 examinations were performed after 12 months during a 1-day visit before the same-day MRI and 2 were performed during treatment of additional aneurysms. The average follow-up interval was 8 months.

Artifact-Related Virtual Stenosis

The minimal diameter of the parent vessel was located at the level of the proximal WEB marker in all cases (Figs 1–4). The susceptibility of the proximal marker resulted in an average virtual stenosis of 38% in TOF-MRA, 33% in CE-TOF, and 13% in UTE-MRI.

Aneurysm Occlusion

Residual filling of the aneurysm adjacent to the WEB device was visible in 8 of 18 cases in DSA, which was used as the criterion standard. The grade of occlusion was 0 in 9 examinations, 0' in 2 exams, 1 in 3 examinations, 2 in 1 examination, 3 in 2 examinations. and 1 + 3 in 1 examination.

With TOF-MRA, 16 of 18 cases were graded correctly. In 2 cases, occlusion was overestimated in TOF (1 instead of 3 and 1 + 3 respectively). With TOF-CE, 16 of 17 cases were graded correctly (1 occlusion overestimation grade 1 instead of 3); and with UTE, 17 of 18 cases were graded correctly (1 occlusion overestimation 0 instead of 0`).

Visualization of the WEB Device and Adjacent Vessels

The visualization of the WEB device position and configuration was rated as good (3) on the UTE sequence in 14 of 18 cases and as intermediate (2) in the remaining 4. Visualization on the TOF sequence was rated as intermediate (2) in 6 patients and poor (1) in the remaining 12 (Figs. 1, 2, and 4). These data are summarized in Table 2.

Statistical Analysis

Interreader reliability regarding all imaging modalities was 0.67 (substantial agreement).

Visibility of the WEB device and adjacent vessels was significantly greater with UTE (median: 3) compared with TOF (median: 2; $P = .008$).

The virtual stenosis was significantly higher in TOF compared with UTE ($P < .001$) and also in CE-TOF compared to UTE-MRI ($P = .003$).

No significant difference in WEB recanalization grading was detected between UTE and DSA ($P = .9$) and between TOF post-contrast and DSA ($P = .45$). A statistically significant difference was present between TOF and DSA ($P = .059$).

DISCUSSION

In this study, we showed that UTE-MRI improves visualization of intra-aneurysmal WEB devices and adjacent vessels compared with routine follow-up MRI with TOF without or with injection of gadolinium-containing contrast media with DSA as the criterion standard. This is shown by the significantly lesser degree of artifact-induced virtual vessel stenosis at the level of the proximal WEB marker in UTE compared with TOF-MRA.

UTE-MRI and TOF-CE performed comparably well in grading of aneurysm recanalization, with TOF-MRA without contrast being slightly inferior; however, this finding did not reach statistical significance.

The main findings of our study are most likely due to the strong susceptibility of the proximal and distal markers of the WEB device. The magnetic field distortion around the markers leads to variations in precessional frequency and subsequently signal loss due to T2* dephasing. This effect leads to severe artifacts on conventional MR imaging, especially gradient-echo sequences such as TOF-MRA. Furthermore, susceptibility artifacts increase with field strength, which is especially relevant for the examination of intracranial aneurysms, in which 3T has been shown to be better than 1.5T.[17,18]

This increase explains the limitations of TOF-MRA in visualization of the WEB device and the adjacent vessels at the aneurysm neck. The higher sensitivity to magnetic field variations is illustrated through the effect of a virtual stenosis in TOF-MRA.

UTE-MRI has a low sensitivity to susceptibility artifacts due to the very short TE, which has been exploited for imaging of the bones and lung parenchyma.[19,20] Several studies have also shown the usefulness of short TE sequences with spin-labelling (Silent-MRA) or IV contrast injection (UTE-MRA) after endovascular introduction of various metallic implants apart from WEB devices. Irie et al[12] demonstrated the use of Silent-MRA in 9 patients treated with stent-assisted coiling with significantly higher subjective visibility compared with TOF imaging. Takano et al[14,15] reported on the use of Silent-MRA in 7 patients treated with Y-configuration stent-assisted coiling and 31 patients treated with Low-Profile Visualized Intraluminal Support (LVIS; MicroVention) stent-assisted coiling, in each case showing substantially better depictability of neck remnant perfusion than on TOF imaging. Oishi et al[13] showed the value of Silent-MRA in visualizing blood flow inside the flow-diverting stent compared with TOF in 78 patients. One study used non-contrast-enhanced sub-UTE-MRA in 6 patients after therapy with a flow-diverting stent and was able to confirm better visualization as well.[21] In addition, time-resolved CEA seems to be beneficial for the follow-up, especially in stent-assisted coil-embolization.[22,23]

Our report showed that combining contrast administration with a UTE sequence is useful for follow-up of intracranial aneurysms treated with the WEB device. Due to the use of IV contrast instead of spin-labelling and subtraction, the structure of the WEB device can be entirely visualized, while not being possible with SILENT-MRA. The most clinically relevant differences compared with TOF were the better ability to depict changes in device configuration that may lead to recanalization and the better ability to judge the patency of parent arteries. Recanalization within the WEB device was not visible with either TOF or UTE MRI and might be due to the inherent magnetic radiofrequency shielding effect.

Depicting the shape and the relation of the WEB device to the parent vessels in noninvasive imaging is relevant, because protrusion of the device requires antithrombotic treatment.[4] The WEB device is designed for broad-based aneurysms; and with increasing operator experience, more complex aneurysms are treated. In highly complex aneurysms with branch incorporation, a certain degree of protrusion is inevitable. This is reflected by the preparation of elective WEB cases with dual antiplatelet therapy by some operators.[4]

UTE-MRI might show benefit as well for the assessment of coiled aneurysms. Even though the susceptibility of coils is inferior compared with the WEB device, small-vessel branches in the vicinity of the coilpack or the parent vessel after stent-assisted coiling can be challenging to evaluate on TOF-MRA.

There are limitations to this study. The number of patients included in this feasibility study is relatively low, increasing the risk of evaluation bias for comparison. The better visibility of the WEB device and the lesser degree of virtual stenosis did not result in changes in patient management in this small feasibility study. Furthermore, no significant difference between UTE and TOF was detected regarding aneurysm occlusion. However, the present study shows that an appropriately powered comparative study regarding aneurysm occlusion would require a larger number of patients.

CONCLUSIONS

UTE-MRI enables more improved visualization of intra-aneurysmal WEB devices than routine follow-up MRI with TOF. The most clinically relevant differences were the ability to judge the patency of vessels at the aneurysm neck and to depict changes in device configuration that may lead to recanalization. Adding UTE MRI to MRI protocols after treatment of intracranial aneurysms treated with the WEB device may be beneficial to depict changes in configuration as well as recanalization and does not excessively extend scan time due to the short acquisition.

REFERENCES

1. Hendricks BK, Yoon JS, Yaeger K, et al. **Wide-neck aneurysms: systematic review of the neurosurgical literature with a focus on definition and clinical implications.** *J Neurosurg* 2019;133:159–65 CrossRef Medline

2. De Leacy RA, Fargen KM, Mascitelli JR, et al. **Wide-neck bifurcation aneurysms of the middle cerebral artery and basilar apex treated by endovascular techniques: a multicentre, core lab adjudicated study evaluating safety and durability of occlusion (BRANCH).** *J Neurointerv Surg* 2019;11:31–36 CrossRef Medline

3. Brinjikji W, Murad MH, Lanzino G, et al. **Endovascular treatment of intracranial aneurysms with flow diverters: a meta-analysis.** *Stroke* 2013;44:442–47 CrossRef Medline

4. Goyal N, Hoit D, DiNitto J, et al. **How to WEB: a practical review of methodology for the use of the Woven EndoBridge.** *J Neurointerv Surg* 2020;12:512–20 CrossRef Medline

5. Larsen N, Fluh C, Madjidyar J, et al. **Visualization of aneurysm healing: enhancement patterns and reperfusion in intracranial aneurysms after embolization on 3T vessel wall MRI.** *Clin Neuroradiol* 2020;30:811–15 CrossRef Medline

6. van Rooij S, Peluso JP, Sluzewski M, et al. **Mid-term 3T MRA follow-up of intracranial aneurysms treated with the Woven EndoBridge.** *Interv Neuroradiol* 2018;24:601–07 CrossRef Medline

7. van Amerongen MJ, Boogaarts HD, de Vries J, et al. **MRA versus DSA for follow-up of coiled intracranial aneurysms: a meta-analysis.** *AJNR Am J Neuroradiol* 2014;35:1655–61 CrossRef Medline

8. Algin O, Yuce G, Koc U, et al. **A comparison between the CS-TOF and the CTA/DSA for WEB device management.** *Interv Neuroradiol* 2022;28:29–42 CrossRef Medline

9. Lubicz B, Klisch J, Gauvrit JY, et al. **WEB-DL endovascular treatment of wide-neck bifurcation aneurysms: short- and midterm results in a European study.** *AJNR Am J Neuroradiol* 2014;35:432–38 CrossRef Medline

10. Akkaya S, Akca O, Arat A, et al. **Usefulness of contrast-enhanced and TOF MR angiography for follow-up after low-profile stent-assisted coil embolization of intracranial aneurysms.** *Interv Neuroradiol* 2018;24:655–61 CrossRef Medline

11. Ozsarlak O, Van Goethem JW, Parizel PM. **3D time-of-flight MR angiography of the intracranial vessels: optimization of the technique with water excitation, parallel acquisition, eight-channel phased-array head coil and low-dose contrast administration.** *Eur Radiol* 2004;14:2067–71 CrossRef Medline

12. Irie R, Suzuki M, Yamamoto M, et al. **Assessing blood flow in an intracranial stent: a feasibility study of MR angiography using a silent scan after stent-assisted coil embolization for anterior circulation aneurysms.** *AJNR Am J Neuroradiol* 2015;36:967–70 CrossRef Medline

13. Oishi H, Fujii T, Suzuki M, et al. **Usefulness of silent MR angiography for intracranial aneurysms treated with a flow-diverter device.** *AJNR Am J Neuroradiol* 2019;40:808–14 CrossRef Medline

14. Takano N, Suzuki M, Irie R, et al. **Usefulness of non-contrast-enhanced MR angiography using a silent scan for follow-up after y-configuration stent-assisted coil embolization for basilar tip aneurysms.** *AJNR Am J Neuroradiol* 2017;38:57–81 CrossRef Medline

15. Takano N, Suzuki M, Irie R, et al. **Non-contrast-enhanced silent scan MR angiography of intracranial anterior circulation aneurysms treated with a low-profile visualized intraluminal support device.** *AJNR Am J Neuroradiol* 2017;38:1610–16 CrossRef Medline

16. Caroff J, Mihalea C, Tuilier T, et al. **Occlusion assessment of intracranial aneurysms treated with the WEB device.** *Neuroradiology* 2016;58:887–91 CrossRef Medline

17. Gibbs GF, Huston J 3rd, Bernstein MA, et al. **Improved image quality of intracranial aneurysms: 3.0-T versus 1.5-T time-of-flight MR angiography.** *AJNR Am J Neuroradiol* 2004;25:84–87 Medline

18. Kwak Y, Son W, Kim YS, et al. **Discrepancy between MRA and DSA in identifying the shape of small intracranial aneurysms.** *J Neurosurg* 2020;134:1887–93 CrossRef Medline

19. Robson MD, Gatehouse PD, Bydder M, et al. **Magnetic resonance: an introduction to ultrashort TE (UTE) imaging.** *J Comput Assist Tomogr* 2003;27:825–46 CrossRef Medline

20. Bergin CJ, Pauly JM, Macovski A. **Lung parenchyma: projection reconstruction MR imaging.** *Radiology* 1991;179:777–81 CrossRef Medline

21. Ayabe Y, Hamamoto K, Yoshino Y, et al. **Ultra-short echo-time MR angiography combined with a subtraction method to assess intracranial aneurysms treated with a flow-diverter device.** *Magn Reson Med Sci* 2023;22:117–25 CrossRef Medline

22. Boddu SR, Tong FC, Dehkharghani S, et al. **Contrast-enhanced time-resolved MRA for follow-up of intracranial aneurysms treated with the Pipeline embolization device.** *AJNR Am J Neuroradiol* 2014;35:2112–18 CrossRef Medline

23. Choi JW, Roh HG, Moon WJ, et al. **Time-resolved 3D contrast-enhanced MRA on 3.0T: a non-invasive follow-up technique after stent-assisted coil embolization of the intracranial aneurysm.** *Korean J Radiol* 2011;12:662–70 CrossRef